Wear tests on PTFE+pb linings for linear pneumatic actuator guide bushings

WEAR TESTS ON PTFE+PB LININGS FOR LINEAR PNEUMATIC ACTUATOR GUIDE BUSHINGS

E. Goti L. Mazza A. Manuello Bertetto

Department of Mechanical and Aerospace Engineering, Politecnico di Torino

ABSTRACT

Guide bushings for linear actuators are subject to intense mechanical stress and wear, especially when external radial forces are applied. Carrying out simplified wear tests on the materials used in these bushings is important in making it possible to estimate how many cycles the actuator can perform before the bushing must be replaced. This paper presents the results of tribological pin-on-disk testing on an anti-friction lining consisting of a porous bronze sinter impregnated and coated with PTFE+Pb. Test specimens were worn with a steel ball, and wear and friction coefficients were determined experimentally with increasing loads and speeds.

Keywords: guide bushings; linear actuators; PTFE+Pb; pin-on-disk; wear coefficient.

1 INTRODUCTION

Linear pneumatic actuators are mechanical units that can convert the energy in a pressurized fluid (compressed air) into mechanical energy, i.e., linear motion. They are widely used in many industrial applications. This type of actuator features a cylinder-piston configuration: the fluid introduced into the chamber exerts a driving force on the piston, causing the rod connected to the load to extend (Fig. 1).

At the actuator front end plate, the rod is supported and maintained in axis with the cylinder by means of a sliding guide bushing consisting of low-friction material. Together with the piston sealing rings, the guide bushings are the components subject to the highest mechanical stress [1] when external radial forces are applied to the rod, as the constraint reactions act on them. The guide bushings are thus more subject to wear than the actuator's other guide components, as they are the smallest of these components and have the highest reaction forces.

Bushing wear causes the rod and cylinder to go out of alignment, resulting in asymmetric overloading and rapid deterioration of the pneumatic seal housed in the front-end plate, which is provided to ensure that the front chamber is airtight (see Fig. 1)

[redacted]

The seal is thus forced to operate in an anomalous configuration [1]. When wear becomes excessive, compressed air leaks from the cylinder end plate. At this point, the guide bushing has reached the end of its service life, and it must be replaced so that the system is usable once again.

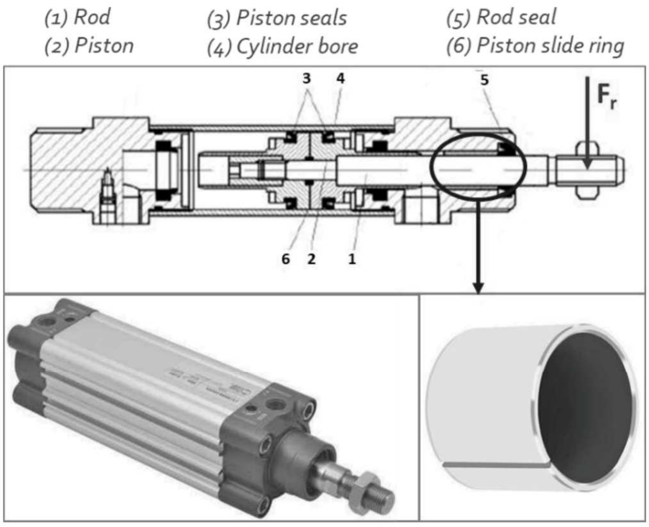

Figure 1 Mechanical layout of a pneumatic actuator

The guide bushing wear process is usually investigated by means of component tests. Ambu et al. [2] carried out accelerated life tests to determine the influence of bushing seat design on the pressure distribution at the bushing/rod interface and the resulting wear.

An approach of this kind, however, entails certain complications: 1) to evaluate the state of wear, the actuator entire plate must be disassembled repeatedly, which inevitably changes the tribological conditions; 2) the component's cylindrical geometry makes it difficult to access the contact region in order to measure the volume of material removed by wear. To simplify tribological testing in mechanical components, the so-called "model tests" as per DIN 50322:1986 [3] have great potential. Nevertheless, it cannot be taken entirely for granted that the behaviour observed for the same materials during simplified tests will be representative of the behaviour of the component in actual service. For guide bushings, it would be extremely useful to be able to predict how many cycles the actuator can perform before it is necessary to replace the bushing without having to test the latter in operation.
The preliminary study presented herein is the first step towards achieving this ambitious goal [4]. The study employs pin-on-disk tests to determine the wear law of a commercial PTFE+Pb based material used as a anti-friction lining for linear pneumatic actuator guide bushings. Tests were carried out on the material, attempting to simulate the worst-case conditions for the component in service. The wear coefficient was thus determined under varying loads and sliding speeds in order to investigate the influence of individual test parameters on material response.

2 MATERIALS AND METHODS

The material selected for this study is marketed by GGB Bearing Technology (Annecy, FR) under the trademark DU®. It consists of a 1.25 mm thick steel backing with a PTFE-based anti-friction lining made up of two superimposed layers: the innermost layer is a porous bronze sinter impregnated with Pb-filled PTFE. The outer sliding layer consists of a 30-50μm thickness of the same polymer composite. The microsection is shown schematically in Fig. 2, compared to the observation of the lining cross-section under the optical microscope in Fig 3. Wear resistance is ensured by the bronze sinter, while the polymer composite provides a self-lubricating effect. Overall thickness is around 300μm and the measured surface roughness is 0.61μm.

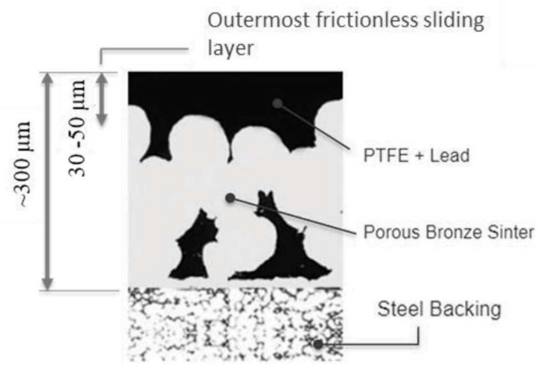

Figure 2 Lining microsection structure from GGB DU® technical sheet.

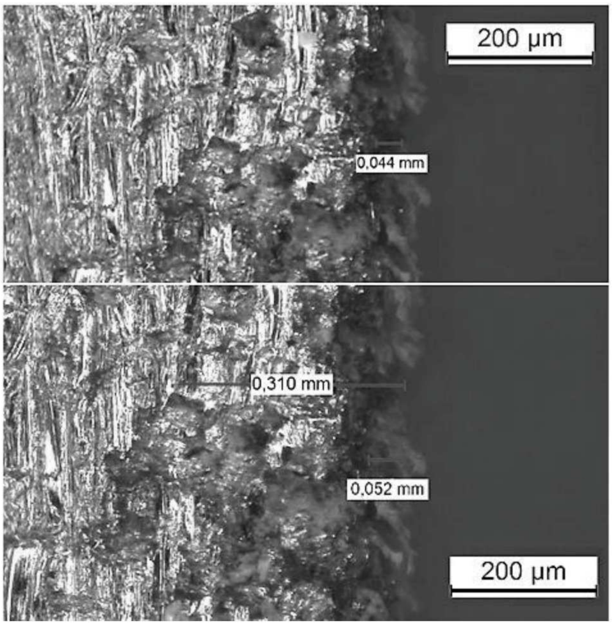

Figure 3 PTFE+Pb lining microsection under the optical microscope

Vickers microhardness (NOVA 130/240, Innovatest), Brinell hardness tests (NEMESIS 9000, Innovatest) and Shore D hardness tests (Sauter Gmbh) were performed on the GGB specimens. As a comparison, the same tests were performed on pure PTFE in order to evaluate the effect of the reinforcing bronze sinter matrix. The relative increase in the hardness value correlates with the desired strengthening effect. Test specimens (Fig. 4b) were cut from flat sheets of the material which is then stamped and drawn to produce the commercial bushings (Fig. 4a).

Table I - Hardness value of the composite polymer-metal lining and comparison with pure PTFE

	Composite lining		Pure PTFE	
Shore D	90.3		52.8	
Vickers microhardness	3.70 HV/0.025	0.036 GPa	2.73 HV/0.025	0.027 GPa
Brinell hardness	15.8 HB2.5/6.25		3.66 HB2.5/6.25	

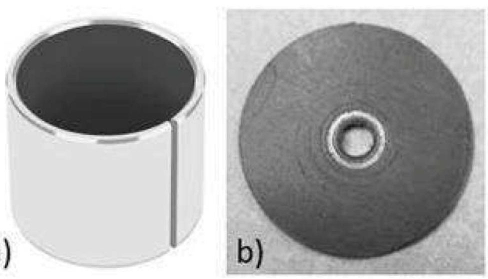

Figure 4 (a) GGB DU® bushing; (b) Test specimen cut from a sheet of the same material.

Tribological tests were carried out on a pin-on-disk rotary tribometer (TRB, Anton Paar) using a 6mm diameter 100Cr6 steel ball. Testing took place in two phases:

- Phase I investigated the effect of normal load. Load was applied in increasing increments of 5 N, 10 N and 20 N, to generate a mean contact pressure of 103 MPa, 130 MPa and 149 MPa respectively. The simulated contact pressures in the most highly stressed area of bushings during service on an actuator are slightly lower [5] but running tribological tests under lower load would have caused pin instability (i.e. pin bouncing) and would have required longer-lasting tests to have enough wear. Sliding speed was maintained constant at 0.3m/s, which corresponds to the mean rod extension speed used in the accelerated life tests presented by Ambu et al. [2]. To take the natural dispersion of wear into account, tests were repeated three times for each load level using the same parameters.
- In phase II, the normal load was maintained constant at the intermediate level of 10N, and sliding speed was increased to 0.5m/s and 0.7m/s. A single test was carried out for each speed increment.

The specimen was replaced at each test in order to maintain a constant wear track radius of 19mm. A total of 12 specimens were required to complete all of the tests described above. Given the modest specimen thickness, it was decided to work only on the outermost portion of the disks, i.e., the portion closest to the point where the disk is supported on the tribometer spindle, to avoid any effect due to flexing under load. Ball-against-flat contact pressure were calculated by means of the Johnson-Kendal-Robert (JKR) model suitable for soft adhesive material [6].

$$p(x) = \frac{3Ka}{2\pi R}(1-x^2)^{\frac{1}{2}} - \left(\frac{3KW_{ad}}{2\pi a}\right)^{\frac{1}{2}}(1-x^2)^{-\frac{1}{2}} \qquad (1)$$

where:

$$a^3 = \frac{R}{K}\left(F_\perp + 3\pi R W_{ad} + \sqrt{6\pi R F_\perp W_{ad} + (3\pi R W_{ad})^2}\right)$$

$$\frac{1}{K} = \frac{3}{4}\left[\frac{1-v_1^2}{E_1} + \frac{1-v_2^2}{E_2}\right]$$

$$W_{ad} = c(E_{s,1} + E_{s,2})$$

Being $E_{s,1}$ and $E_{s,2}$ the surface energy of PTFE and steel respectively (estimated from literature data [7]), E_1 and E_2 the corresponding Young module, c the coefficient of compatibility and W_{ad} the specific work of adhesion. Table II lists the value of the quantities used in the JKR equations. Young module was measured by instrumented indentation (MCT, Anton Paar) with a Vickers diamond indenter. Continuous-multi-cycle (CMC) indentation mode allowed to explore the evolution of the mechanical properties with increasing the penetration depth, due to the multi-layered structure of the lining. The diagram in Fig.5 shows that the elastic modulus takes a stable value of 1.2 GPa down to about 15um depth. Hardness has a similar trend with an average value of 0.03GPa. Beneath, the values start increasing due to the influence of the stiffer bronze matrix. The Young modulus value to be used as inputs to the JKR equation was identified as the average of the measured values up to a penetration depth equal to the position of the maximum Von Mises stress, by means of an iterative procedure.

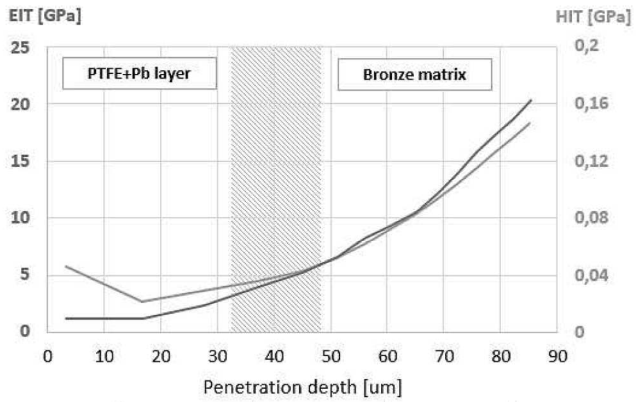

Figure 5 Elastic modulus (EIT) and instrumented indentation hardness (HIT) versus indentation depth

Table II - Surface properties involved in the pressure calculation according to the JKR model

Physical quantity	Value	Units
E_1 (lining)	4.75	GPa
E_2 (steel)	210	GPa
v_1 (PTFE)	0.46	-
v_2 (steel)	0.3	-
$E_{s,1}$ (PTFE)	0.018	J/m2
$E_{s,2}$ (steel)	0.9	J/m2
c	0.12	-
W_{ad}	0.11	J/m2
K	807.3	MPa

Tribological tests were run for an accumulated sliding distance of 4000m, stopping at regular intervals to measure wear volume: every 150m up to the first 900m; then every 500m up to the total envisaged sliding distance. Wear volume was measured as per ASTM G99-17 [8], where volume loss is estimated by applying Guldino's theorem.

$$V = 2\pi \cdot r \cdot A \qquad (2)$$

where A is the average wear track cross section area and r is the track radius (i.e., the distance of its geometric centroid from the axis of revolution). As directed in the standard, the three wear depth profiles were measured using a stylus profilometer (PGS2000, SM Metrology System) and *A* was determined by averaging the areas of each wear scar profile.

3 RESULTS AND DISCUSSION

3.1 RESULTS OF PHASE I

Fig. 6 shows the results for stage I of this study. The values shown refer only to wear on the sample, as there was no measurable wear on the ball because of its greater hardness. Each plot shows wear volume versus sliding distance for the tests carried out at the same normal load (grey curves). As indicated above, the wear volume at each interruption was calculated by measuring three wear depth profiles at randomly selected locations. However, cross-section area measurements showed considerable scatter because of the wear scars' highly irregular configuration. During data analysis, it was thus decided to treat any of the three values that departed excessively from the other two as outliers. In hindsight, it would have been better to use a larger number of depth profiles rather than the three suggested by the standard in order to estimate volume loss more effectively.

Fig. 6 also shows mean wear volume (black curve), plotted by averaging the values for each curve at each test interruption.

Even under 20N load, the pin never penetrated sufficiently to remove all of the anti-friction layer and contact the steel backing, a condition which would have made it pointless to continue the test.

As can be seen from these average curves, volume loss does not increase uniformly, as is typically the case for many bulk materials [7]. With reference to these curves, the following points should be noted:

- Initial wear-in with nonlinear volume loss always ends within the first 150m and is not visible because of the selected interruption intervals. After the first 150m, wear increases more or less linearly with a steep slope. This represents the first wear stage (corresponding to the orange linear fits in Fig.6)

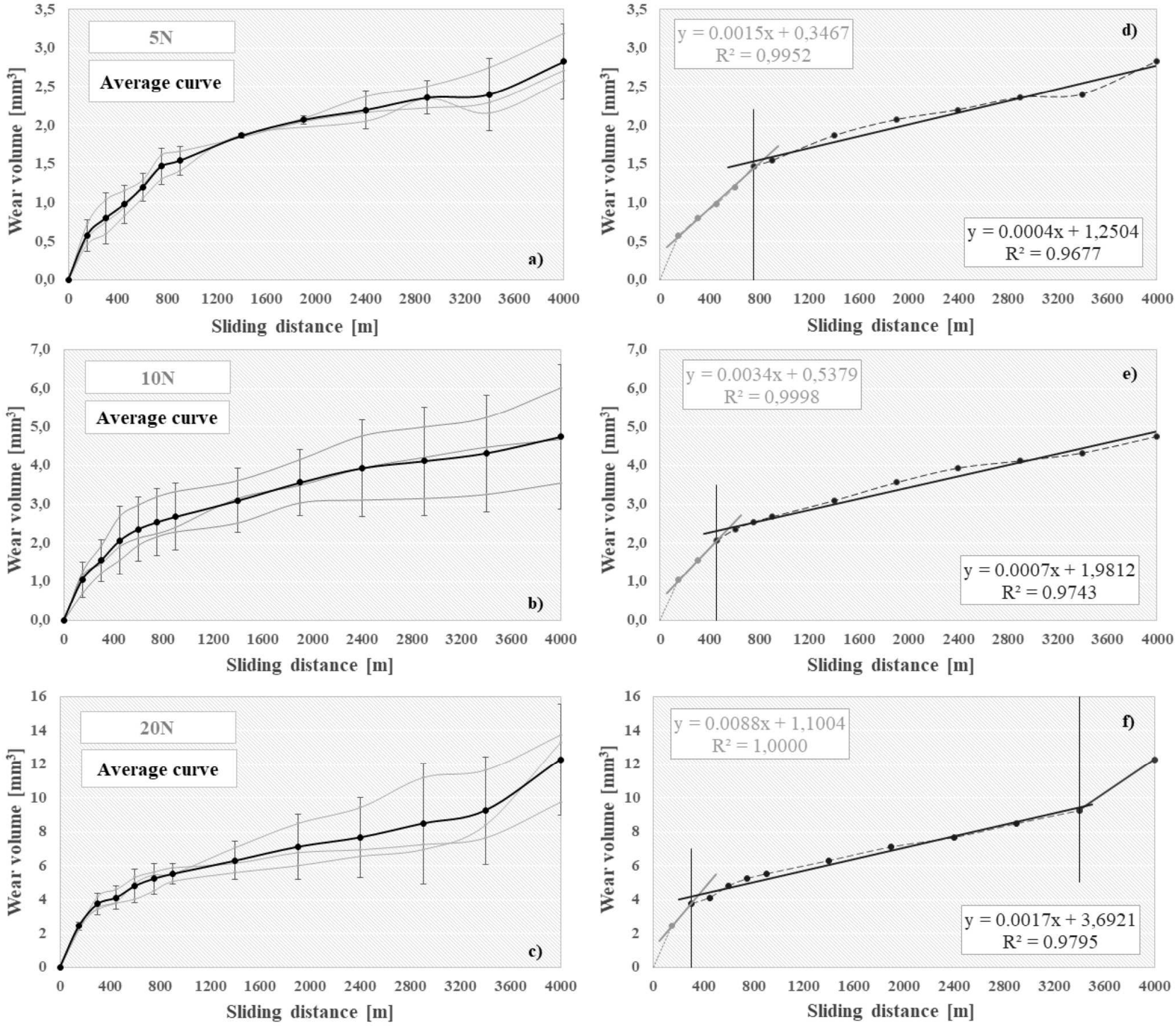

Figure 6 (a), (b), (c) Average wear volume compared to individual tests at the same normal load (grey) and the corresponding uncertainty represented as error bars calculated as 3 times the standard deviation at each interruption; (d), (e) and (f) Piecewise linear fit curve for the average volume loss.

- Upon reaching a certain distance between 300m and 750m, there is a transition to a second, flatter slope where the trend is still linear. The point of transition towards this second wear stage (indicated by the vertical line) varies according to load and takes place at shorter sliding distances as load increases. This transition is likely to be due to the structure of the anti-friction lining illustrated in Fig. 2 and corresponds to the operating performance declared in the bushing manufacturer's datasheet.

In the first part of the test, wear is concentrated in the PTFE+Pb layer. In this stage, the pin contacts the bronze sinter occasionally at most, so it is natural to expect volume loss to increase rapidly. PTFE and its composites have low coefficients of friction, but also low abrasion resistance [7] [9], [10].

The transition to a flatter linear slope (stage 2) marks a condition where pin penetration is sufficient to bring the ball into contact with the layer where the bronze sinter is impregnated with the polymer composite.

Lining damage proceeds more slowly because of the supporting effect of the bronze globules, which are more wear resistant. Wear rate increased again between 3400m and 4000m only in the 20N test. This could be due to a wear mechanism transition associated with an increase in the ball area in continual contact with the deeper bronze layer.

This experimental behaviour is consistent with what is expected based on the GGB DU® bushing technical sheet. Fig. 7 is an extract from the technical sheet which represents the evolution of the bushing damage against a rotating shaft.

It is obvious that the wear volume trend is very similar to the one experimentally measured by sliding pin-on-disk-tests and similar wear stages appear as well, at a different time-scale though.

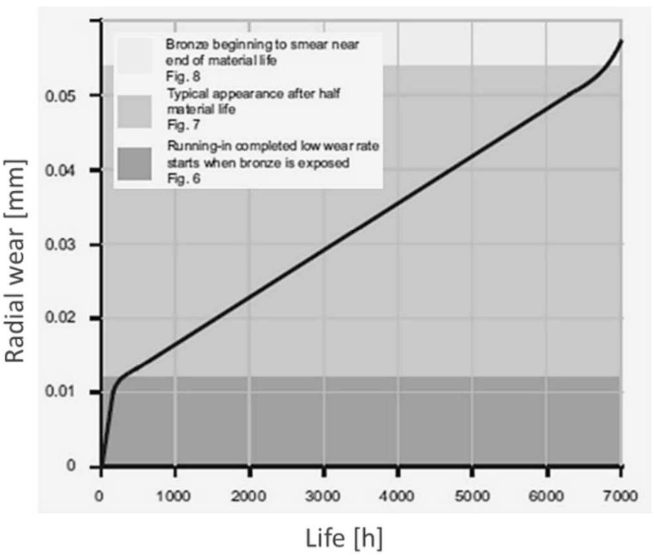

Figure 7 Wear curve as per GGB DU technical sheet.

Table III summarizes the wear rates for the analysis pictured in Fig. 6. The wear rate is defined as the ratio of the change in volume loss to the increase in the length of the interaction $\partial V/\partial l$, and according to Archard's linear law [11] is the slope of the line describing the experimental wear curve. The table also shows the Archard wear coefficients calculated as

$$K = (V/L) \cdot (H/F_N) \tag{2}$$

where (V/L) is the wear rate identified from the linearized experimental wear curves, H is the material Vickers microhardness and F_N is the applied load.

Table III - Experimental wear coefficients K

Load	Stage	V/L [mm^3/m]	K [adimens.] [SI]	I→II
5N	1	0.0015	$1.11 \cdot 10^{-05}$	750m
	2	0.0004	$2.97 \cdot 10^{-06}$	
10N	1	0.0034	$1.26 \cdot 10^{-05}$	450m
	2	0.0007	$2.60 \cdot 10^{-06}$	
20N	1	0.0088	$1.63 \cdot 10^{-05}$	300m
	2	0.0017	$3.16 \cdot 10^{-06}$	

In stage 2 the increase in the wear rate is approximately proportional to the load (wear rate doubles when load is doubled, and again when load is quadrupled) so that K oscillated around a mean value of about $3 \cdot 10^{-06}$.

In stage 1, by contrast, the increase is not proportional in passing from 10N to 20N: when the applied load is doubled, the wear rate triples. This leads to an almost 50% increase in K over the constant value at 5N and 10N.

It should be emphasized that the transition points shown in Fig. 6 are indicative, and there is a certain scatter from specimen to specimen which is also influenced by the uncertainty in estimating the volume loss.

In addition, the very nature of the lining and the inevitable variability in its composition 'blur the boundaries' dividing the first and second stages of wear (i.e., layers).

Profilometric data and optical microscope inspection of wear tracks confirmed that the position of the transition points of wear curves corresponds to the transition between layers of the lining.

The image of the wear track upon interrupting the test immediately after the transition shows that the density of bronze globules exposed by ball action is greater than that visible before the transition. An example for a test under 5N load with transition at approximately 750m is shown in Fig.8.

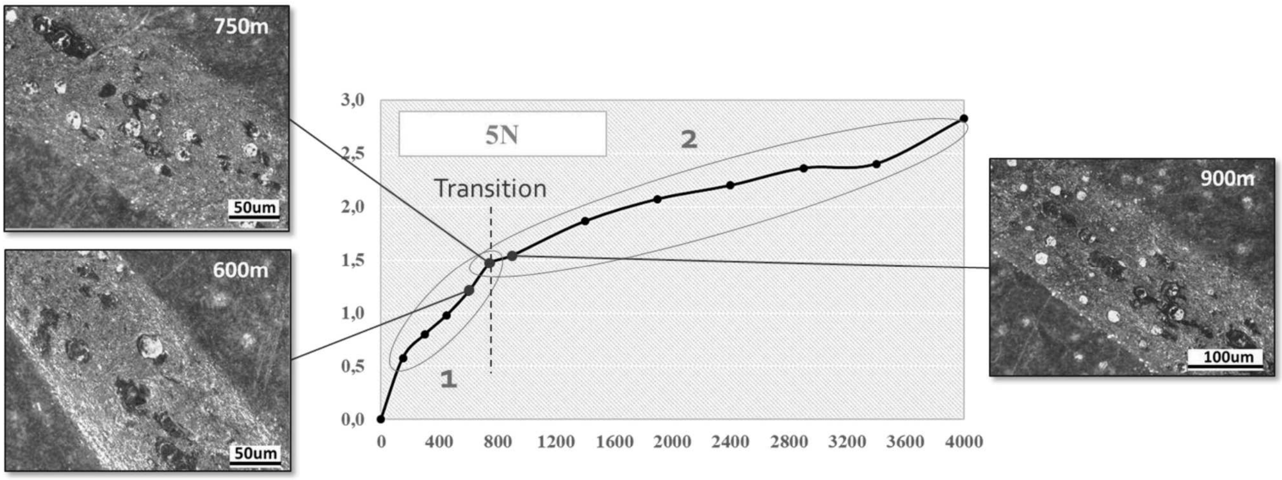

Figure 8 Optical microscope images of wear track in a test 5N test. At the transition (750m), the number of bronze globules in the underlying layer exposed by wear increases.

As to profilometry, the identified transition points correspond to a maximum wear track depth of about 25-30um, which is consistent with the measured limit of the outer PTFE+Pb layer. The friction coefficient was measured during the wear tests as well to assess any possible correlations with wear behaviour. Fig. 9 shows the mean friction curves plotted by averaging data for each test with the same applied load. The curves ragged appearance is due to the repeated interruptions needed in order to determine the volume loss. At each interruption, the wear debris was removed from the specimen, and the latter was taken off the tribometer to measure the wear depth profiles. Each outside intervention on the system inevitably changes the state of the interface, which is why the friction coefficient drops momentarily each time testing is resumed. As Holmberg [1] notes, such behaviour is commonly observed in start/stop situations. For the most part, the interaction between the ball and the polymer lining is stable throughout the test (curves are almost horizontal). The average value drops slightly from 0.176 for the tests at 5N to 0.153 at 20N, while the initial run-in stage ends after 30-70m at 5N and after 15-25m at 20N.

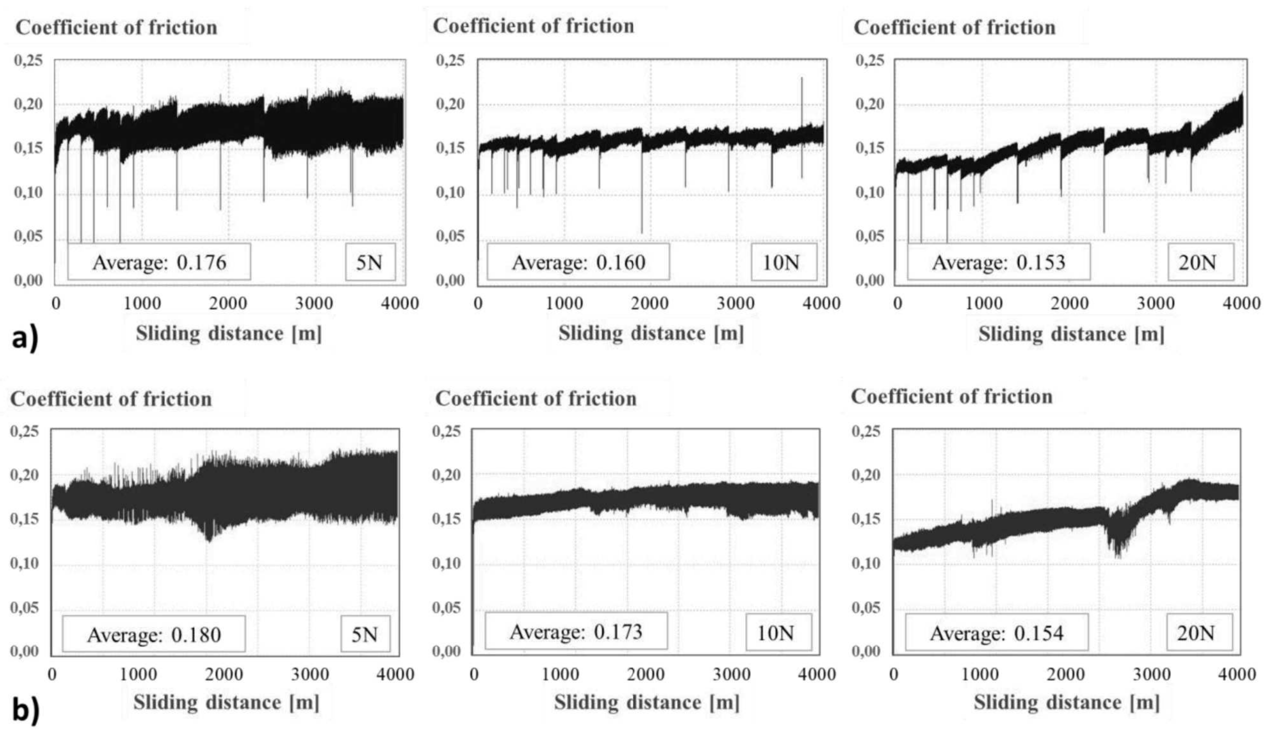

Figure 9 Average friction measured (a) during periodically stopped pin-on-disk wear tests, (b) during continuous pin-on-disk tests.

The friction coefficient thus stabilizes long before the ball begins to wear the deepest layer, demonstrating that the PTFE compound has the same beneficial effect even when used as a filler in the bronze sinter.
The average friction curves are compared to the ones measured in same conditions without stopping the test at regular intervals. The curves are rather similar as well as the average CoF, so that stopping the test should not have much impact on the tribological behaviour of the lining, as far as friction is concerned at least.
The measured friction coefficient perfectly agrees with the behaviour reported by the GGB DU® technical sheet according to which a thin PTFE transfer layer should grow on the rigid counterpart (i.e. the ball) preventing direct metal-bronze contact.
In these tests the specimens were cleaned from debris at each stopping to take the profile measurements, unlike the ball whose wear damage was negligible. This also suggests that pneumatic actuator guide bushings employing this material would operate effectively with low friction force even under severe wear damage at the point of highest stress. As a consequence, the tribological and functional end-of-life of the bushings may not coincide and the coefficient of friction is not necessarily an indicator of the loss of functionality of the bushing, at least for what has been observed so far.
The 20N tests are the only ones were the wear coefficient shows an upward drift after 3500m. This further sharp increase in the coefficient which coincides approximately with the second wear volume transition (Fig. 4), visible only in these tests.
It can thus be hypothesized that there is a correlation between this increase in friction coefficient and the increase in wear coefficient, both being due to the predominance of bronze in the contact interface.
Longer-lasting pin-on-disk tests under 5N, 10N and 20N will be useful to verify the presence of a late transition in the friction and wear curves to be regarded as a characteristic of this lining. If verified, it could be inferred either that the lubricating effect of the PTFE+Pb transfer layer tends to disappear at greater depths or that a new wear mechanism is arising.

3.1 RESULTS OF PHASE II

Fig. 10 shows the volume loss curves for two tests at sliding speeds of 0.5m/s and 0.7m/s. These curves are compared with the average wear curve for the three tests carried out at 10N and 0.3m/s during phase I. Volume loss increase is very similar for all three curves, with the transition knee between stage I and stage II located around 450m for all sliding speeds.
Bearing natural scatter in mind, we can say that sliding speed has no influence on lining wear performance in the investigated range. Friction curves do not show significant differences with increasing sliding speed as well (see Fig. 10b).

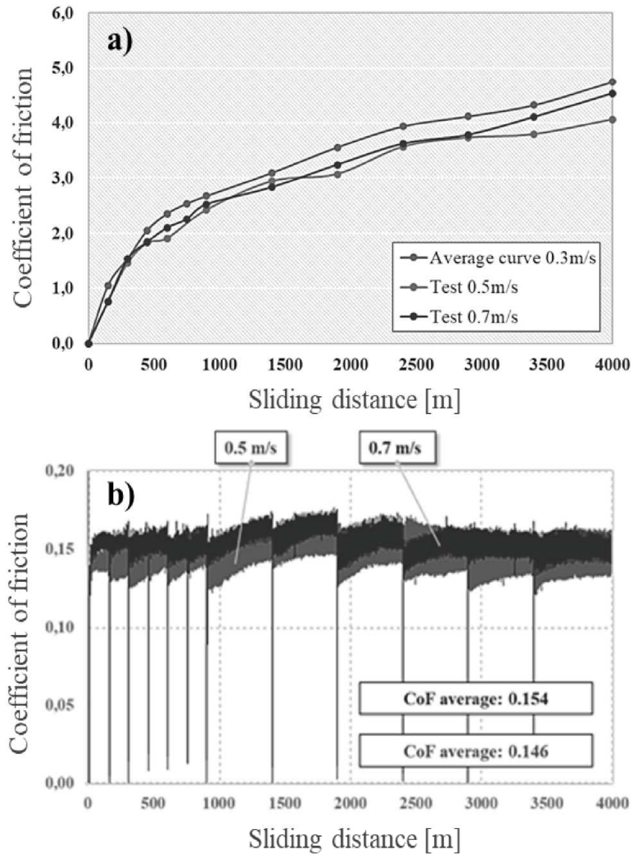

Figure 10 (a) Volume loss versus sliding speed; (b) corresponding friction curves under increased sliding speed

4 CONCLUSIONS

For the study presented herein, a composite PTFE+Pb and bronze lining was worn against a steel ball using a pin-on-disk test setup. In the first phase of testing, load was varied at constant speed, while in the second phase speed was varied at constant load.
Measuring volume loss under increasing load made it possible to identify two stages in the wear process, both of which were linear. In stage 1, the wear coefficient is 4 to 5 times higher than in stage 2, which can be attributed to the fact that the latter reaches the innermost layer of the lining where the PTFE+Pb composite is reinforced by the bronze sinter. Load affects the wear coefficient at least in the first stage. In both the first and second stages of wear, the friction coefficient remains stable with an average that drops slightly as applied load is increased. A further sharp increase in both the wear coefficient and the friction coefficient after 3500m was observed only in the test with 20N load, probably because bronze predominates over the PTFE at greater depths. This hypothesis can be confirmed only by carrying out further tribological tests with applied loads of 5N and 10N and increased sliding distances in order to determine whether the same type of transition occurs for similar pin penetrations.

It would also be interesting to carry out future tests to determine whether this particularly severe lining wear condition can be correlated with the pneumatic actuator end-of-life condition identified by Ambu et al. [2].

Pin-on-disc tests revealed a wear volume trend similar to what the manufacturer stated and similar to the trend obtained from accelerated life tests.

This result is encouraging but the comparison with latter data is not straightforward. A method should be developed for extrapolating bushing life (measured in hundreds of km, see [2]) on the basis of the sliding distance measured in thousands of meters in pin-on-disk tests.

The point of transition in the wear curves of bushings occur at higher radial wear values than the pin penetration in pin-on-disk tests and even the steel backing is likely to be affected by wear, at least in the most stressed region of the bushing. This supports the hypothesis that the functional end of the bushings does not coincide with the tribological end-of-life of the lining, and friction coefficient cannot be used as an indicator for the first.

The results of the second experimental phase show that sliding speed is a minor parameter. Doubling the sliding speed results in no change in the volume loss curve, at least in the speed range and conditions used in this study.

By contrast, other experimental data reported in the literature (e.g. [7]) indicate that speed is a critical parameter for polymer materials because of the temperature increase it causes at the interface.

In these tests, the temperature increase at the interface may have been limited by the frequent interruptions needed to measure the wear depth profiles and the bronze matrix could also have played a role.

It is worth therefore to further investigate the effect of speed with continuous test runs, checking whether there are differences in the volume of removed material in the presence and in the absence of repeated interruptions of tests.

REFERENCES

[1] Belforte G., Raparelli T., Mazza L., Analysis of typical component failure situations for pneumatic cylinders under load, *Lubrication Engineering,* vol. 48, pp. 840-845, 1992.

[2] Ambu R., Manuello Bertetto A., Mazza L., Re-design of a guide bearing for pneumatic actuators and life tests comparison, *Tribology International,* 96 (2016) 317-325.

[3] "DIN 50322:1986, DINWEAR - CLASSIFICATION OF CATEGORIES IN WEAR TESTING," DIN Platz, Berlin.

[4] Goti E., Mazza L., Manuello Bertetto A., Prove di usura su rivestimento di PTFE+Pb per boccole guida di attuatori pneumatici lineari, *7° Workshop AIT Tribologia e Industria* (2020), ISBN_9788890818530

[5] Manuello Bertetto A., Mazza L., Orrù P., Contact Pressure Distribution in Guide Bearings for Pneumatic Actuators, *Experimental Techniques,* 39 (2015) 46-54

[6] Zeng H., *Polimer, Adhesion Friction and Lubrication*, John Wiley & Sons, 2013.

[7] Straffelini G., *Friction and wear*, Springer, 2015.

[8] "ASTM G99-17 Standard Test Method for Wear Testing with a Pin-on-Disk Apparatus," ASTM International, West Conshohocken, PA, 2017.

[9] Chaudhari S.B., Shekhawat S.P., Wear Analysis of Polytetrafluoroethylene (PTFE) and its composites under Wet Conditions, *IOSR Journal of Mechanical and Civil Engineering,* vol. 8, No. 2, pp. 7-18, 2013.

[10] Zeng S., Li J., Zhou N., Zhang J., Yu A., He H., Improving the wear resistance of PTFE-based friction material used in ultrasonic motors by laser surface texturing, *Tribology International* 141 (2020) 105910

[11] Archard J.F., Contact and Rubbing of Flat Surfaces, *J. of Appl. Phis.,* vol. 24, pp. 981-988, 1953.

[12] Holmberg K., Matthews A., *Coatings Tribology*, Elsevier Science, 1994.